Submitted to Physical Review C

LBL-2917
Preprint

NUCLEAR ORIENTATION STUDIES OF ^{241}Am AND ^{255}Fm

A. J. Soinski and D. A. Shirley

June 1974

Prepared for the U. S. Atomic Energy Commission
under Contract W-7405-ENG-48

DISCLAIMER

NUCLEAR ORIENTATION STUDIES OF ^{241}Am AND ^{255}Fm†

A. J. Soinski and D. A. Shirley

Department of Chemistry and
Lawrence Berkeley Laboratory
University of California
Berkeley, California 94720

May 1974

ABSTRACT

Nuclei of ^{241}Am and ^{255}Fm were oriented in single crystals of neodymium ethylsulfate at temperatures down to 11 mK. Orientation was detected by α-particle angular distributions. The temperature dependences of these distributions were consistent with the lowest electronic states of these two actinide ions in the ethylsulfate lattice being similar to those of the corresponding lanthanide ions. Thus quadrupole orientation was observed in $Am^{3+}(5f^6)$, as in $Eu^{3+}(4f^6)$. In $Fm^{3+}(5f^{11})$ the orientation was magnetic and equatorial ($|B|>|A|$), as would be expected from the hyperfine interaction in $Er^{3+}(4f^{11})$. For ^{241}Am we report $P = -0.0033(6)$ cm^{-1}, and for ^{255}Fm, $|B| = 0.035(7)$ cm^{-1}. The Am^{3+} data are consistent with an anti-shielding constant of $\gamma_\infty \approx -10^2$, in good agreement with theory, and a shielding factor $\sigma_2 = 0.7$, similar to the value for Eu^{3+}. The nuclear results showed that the s and d alpha particle partial waves are in phase for the favored α-decay branch in each case. The relative phase of the g wave could not be determined.

I. INTRODUCTION

In a previous paper[1] (hereafter designated as I) nuclear orientation results for ^{253}Es substituted into a single crystal of neodymium ethylsulfate (NES) were reported. The expected similarity between the electronic ground states of the analogous lanthanide and actinide trivalent ions, as exemplified by similar hyperfine interaction parameters, was confirmed for the pair Ho^{3+} - Es^{3+}. These simularities were also exhibited in the optical spectra as shown by Carnall et al[2] for Tb^{3+}:$LaCl_3$ and $BkCl_3$.

Nuclei of trivalent ^{152}Eu and ^{154}Eu ions were aligned in NES by means of the electric hyperfine interaction between the nuclear quadrupole moment and the electric field gradient arising from both the open f-electron shell and the lattice charges.[3] Because the lattice charges are farther from the nucleus than the f-electrons, the f-electron contribution to the field gradient was expected to dominate. Since this was not the case, Judd et al[3] proposed that distortion of the closed electronic shells by the lattice charges increased or antishielded the crystal field gradient at the nucleus. This unexpected result suggested that americium should also be studied. Sternheimer[4] and later Gupta and Sen[5] predicted that the lattice antishielding factor, γ_∞, is larger for Am^{3+} than for Eu^{3+}; therefore appreciable alignment of Am^{3+} would be expected. In this paper we report nuclear orientation experiments on ^{241}Am. The data are interpreted in terms of both the crystal field parameters and the relative amplitudes and phases of the alpha waves in the favored decay to ^{237}Np. Our results are compared with those from alpha-gamma angular correlation measurements[6-9] on ^{241}Am and ^{243}Am. The angular correlation data for ^{241}Am give a positive relative s-d wave phase, and the ^{243}Am data set a lower limit on the relative d to s wave amplitude for the favored decay to ^{239}Np.

The most important result of I was the testing of the shell model theory of alpha decay as applied by Poggenburg et al.[10] Although the relative partial wave phases were correctly predicted, the relative intensities were in error. The calculated intensities of both the d and g waves to ground were too small to fit the angular distribution. Our present results do not permit an additional test because the calculated g wave intensity for ^{241} is very small, and the angular distribution is not particularly sensitive to changes in the g wave intensity. As for ^{253}Es, the relative s-d phase in ^{241}Am favored decay is positive.

We also report results for ^{255}Fm in NES.[11] We find that the s and d waves are also in phase in this case. Because of the short half-life (20.1 h) and the limited mass available, the statistical accuracy was not high enough to permit the extraction of the sign of the relative s-g wave phase. The similar electronic ground state of the pair Er^{3+} - Fm^{3+} is confirmed.

II. THEORY

The alpha particle angular distribution function may be expanded in terms of even order Legendre polynomials,

$$W(\Theta) = 1 + \sum_{\substack{k>o \\ \text{even}}} \sum_{\ell,\ell'} a_\ell a_{\ell'} \cos(\phi_\ell - \phi_{\ell'}) Q_k(\Theta) b_k(\ell\ell' I_f I_i) * F_k(\ell\ell' I_f I_i) B_k(I_i, T) P_k(\cos\Theta) \Big/ \sum_\ell a_\ell^2 . \quad (1)$$

Each partial wave amplitude, a_ℓ, is proportional to the square root of the wave intensity to a given daughter level divided by the velocity of the alpha particle populating that level. Methods for obtaining these amplitudes are discussed in the next section. The permitted ℓ-values are determined by the usual vector coupling rule that the nuclear spin of the daughter plus the orbital angular momentum of the alpha particle wave equal the nuclear spin of the parent. Only waves of the same energy can interfere with one another, and hence the summation over ℓ,ℓ' in Eq. 1 is weighted according to the measured total wave intensity to each daughter level. The phase shifts, ϕ_ℓ, can be obtained only from the numerical integration of the coupled differential equations describing the penetration of the alpha particle through the anisotropic potential barrier. However, the quadrupole phase shifts resulting from penetration of the non-central part of the barrier are relatively small. The waves can be taken as completely in phase or out of phase on the nuclear surface, and then shifted by penetration of a pure Coulomb barrier. The product $b_k F_k$ is well-known from angular correlation theory. The Q_k are solid angle factors which account for the finite angular extent of both the source and the detector. The orientation parameters $B_k(I_i,T)$ depend on the populations of the nuclear magnetic substates which in turn depend on the magnitude and nature of the hyperfine interaction and the temperature.

The hyperfine interaction between a rare-earth or actinide nucleus of spin I at a site of crystalline axial symmetry and its surroundings can be described by a spin Hamiltonian[12]

$$\mathcal{H}_{hf} = AI_zS_z + B(I_xS_x + I_yS_y) + P(I_z^2 - I(I+1)/3) \qquad (2)$$

where A and B are magnetic hyperfine interaction constants and P is the quadrupole coupling constant. The magnetic hyperfine interaction has already been discussed in I; we now consider the electric hyperfine (ehf) interaction.

The ehf splitting of the nuclear magnetic substates results from the interaction between the nuclear quadrupole moment, Q, and the electric field gradient (EFG) at the nucleus. In NES there are four sources of an EFG at the rare-earth site: 1). the lattice charges and dipoles, 2). the open f-electron shell, 3 and 4). closed electronic shells that are polarized or distorted by the quadrupole part of the crystal field (CF) potential and by the unfilled f-shell. The resultant EFG may be written as[13]

$$eq = eq_{nf}(1 - R_Q) + eq_{lat}(1 - \gamma_\infty) \qquad (3)$$

where R_Q and γ_∞ are the atomic and lattice Sternheimer[14] antishielding factors respectively. Since the quadrupole interaction is proportional to $\langle r^{-3} \rangle$, the lattice term would usually be smaller than the f-electron term were it not for the enhancement of the quadrupole component of the CF potential resulting from distortion of closed shells.

At a site of axial symmetry the quadrupole coupling constant is

$$P = \frac{3e^2Qq}{4I(2I-1)} = \frac{3eQ}{4I(2I-1)} \frac{\partial^2 V}{\partial z^2} . \qquad (4)$$

The part of the CF potential relevant to the ehf interaction is $A_2^0 (3z^2 - r^2)/-e$. Therefore the lattice contribution to P is

$$P_{lat} = - \frac{3Q(1 - \gamma_\infty)A_2^0}{I(2I - 1)} \tag{5}$$

with the Sternheimer antishielding factor explicitly included.

Am^{3+} has a $5f^6$ electronic configuration outside the radon core. The Hund's rule ground state is $^7F_0$, as in $Eu^{3+}(4f^6)$. Since the ground state is a singlet, there is no magnetic hyperfine interaction. The f-electron contribution to P was calculated by Elliott[15] using second order perturbation theory. He considered the admixture of the J = 2, J_z = 0 electronic state into the ground state to obtain

$$P_{5f}^{(2)} = \frac{6e^2Q\, A_2^0\, (1-\sigma_2)\, \langle r^2 \rangle_{5f}\, \langle r^{-3} \rangle_{5f}\, (1-R_Q)\, |\langle 20\|\alpha\|00 \rangle|^2}{I(2I-1)\, E(^7F_{20} - {}^7F_{00})} \tag{6}$$

The ionic shielding parameter σ_2 gives the shielding of the 5f-electrons from the crystal field by the outer electrons, primarily the 6s and 6p shells. The reduced matrix element results from the application of operator equivalents in the evaluation of matrix elements of potential operators.

III. RESULTS AND DISCUSSION

The coefficient of each Legendre polynomial in Eq. 1 can be factored into (an $A_k(\ell\ell' I_f I_i)$ term depending on the spins and multipolarities involved in the decay) times (a $B_k(I_i, T)$ term depending on the hf interaction of the nucleus with its environment and the temperature). Thus if the temperature is known, independent information can be obtained about both the hf interaction mechanism and the alpha wave amplitudes and phases. First a value of P, as

derived from the temperature dependence of the angular distribution, will be interpreted. Then the dependence of $W(\theta)$ on the partial wave amplitudes and phases will be discussed.

The experimental ^{241}Am alpha particle angular distribution measured at 0° and 90° with respect to the NES c-axis as a function of the inverse temperature is shown in Fig. 1, and the results are tabulated in Table I. The numbers shown in parentheses for $W(\theta)$ are the standard deviations based on counting statistics. The inverse temperatures have a possible error of 6% in addition to any error shown in parentheses. Details of the experimental technique have been given in I. The linear temperature dependence of $W(\theta)$ at higher temperatures is characteristic of electric quadrupole alignment. If the $P_4(\cos\theta)$ term in Eq. 1 is small, the angular distribution function reduces to

$$W(\theta) = 1 + A_2(\ell\ell' I_f I_i) Q_2 B_2(I_i, T)(3\cos^2\theta - 1)/2. \qquad (7)$$

and $B_2(I_i, T) \propto 1/T$ at high temperatures for quadrupole alignment. For the series of adiabatic demagnetizations reported here $Q_2(0) = 0.930$, $Q_4(0) = 0.787$, $Q_2(\pi/2) = 0.955$, and $Q_4(\pi/2) = 0.855$.

In order to determine accurately the value of P it is necessary that the temperature be low enough such the $P \approx kT$, where k is Boltzmann's constant. Then curvature develops in the $W(\theta)$ vs. $1/T$ curve. Since sufficiently low temperatures were not possible using NES as a host, our value for P of -0.0033(6) cm^{-1} (P/k = -0.0048(8)K) lacks precision. The negative sign implies that the nuclear magnetic substates $I_z = \pm 5/2$ lie lowest in energy.

In the analysis of the nuclear orientation of ^{152}Eu in NES[3] P_{4f}[2] could be calculated with reasonable accuracy because the value of the CF parameter $B_0^2 = 2A_2^0(1-\sigma_2)\langle r^2 \rangle_{4f}$ had been experimentally determined. A value for σ_2 was then calculated. Although B_0^2 for Am^{3+} has not been determined, we can make a reasonable estimate and then proceed with the analysis. We write

$$P_{expt.} = -\frac{3QB_0^2}{2I(2I-1)}\left[\frac{1-\gamma_\infty}{\langle r^2 \rangle_{5f}(1-\sigma_2)} - \frac{2e^2\langle r^{-3} \rangle_{5f}(1-R_Q)\,|\langle 20\|\alpha\|00 \rangle|^2}{E(^7F_{20}-{}^7F_{00})}\right]. \quad (8)$$

Every term on the right hand side of Eq. 8 either is known or can be estimated with reasonable accuracy except for B_0^2, σ_2, and R_Q. We discuss R_Q first and then return to the CF terms.

The atomic Sternheimer factor R_Q accounts for the shielding of the f-electron generated field gradient by the closed electron shells as measured at the nuclear site. For the lanthanides R_Q is of the order of 0.08 - 0.13 (Ref. 5) and therefore shielding. However Sen[5] calculated a value of R_Q = -0.087 for Am^{3+} as a free ion. This is in contrast to the experimental value of $R_Q = 0.35(10)$ for Np^{6+} (Ref.16). R_Q is not expected to be strongly dependent on either Z or the ionic charge within a period; however, ion-ligand overlap is important for the spatially extended 5f-electrons. Therefore the disagreement between the experimental and theoretical values is not surprising. We accept the value of $R_Q = 0.35$ as being valid for Am^{3+}. We shall find below that the second expression in brackets in Eq. 8 is smaller than the first; therefore our conclusions are not affected by this choice.

There have been two determinations of B_0^2 for trivalent actinides at trigonal sites. For $LaCl_3:Am^{3+}$ Gruber[17] obtained $B_0^2 = 412\ cm^{-1}$. However, the J-levels in the optical spectra were not properly assigned,[18] and therefore this value may be in error. For $LaBr_3:Np^{3+}$ Krupke and Gruber[19] obtained $B_0^2 = -22.8\ cm^{-1}$ which indicates a value for σ_2 greater than one since A_2^0 should be positive for the actinides. This agrees with both the large values of σ_2 reported for the light rare earths by Blok and Shirley[20] and the calculations of Gupta and Sen.[5] Sengupta and Artman[21] calculated $\sigma_2 = 0.881$ for Np^{3+} whereas Sen[5] calculated $\sigma_2 = 1.091$ for Am^{3+}. Therefore the theoretical calculations do not firmly establish the sign of σ_2 and hence the sign of B_0^2 for Am^{3+}. Carnall[22] has suggested that the negative B_0^2 for $LaBr_3:Np^{3+}$ may be the result of using a model that is not sufficiently refined and that σ_2 should be less than one for both Np^{3+} and Am^{3+}. Preliminary analyses of the optical spectra of Nd^{3+} and U^{3+} yielded $B_0^2(U^{3+}) \approx 3\text{-}4\ B_0^2(Nd^{3+})$.[23] If, as a working estimate, we take $B_0^2(Am^{3+}) = 4B_0^2(Eu^{3+})$, then $B_0^2(Am^{3+}) = 640\ cm^{-1}$ using $B_0^2(Eu^{3+}) = 160\ cm^{-1}$ (Ref. 24).

We can now calculate $1 - \sigma_2$ using Eq. 8. The ^{241}Am quadrupole moment is 4.9 b. (Ref. 25). The Sternheimer factor $1 - \gamma_\infty$ is calculated to be 112.92,[5] a value which should be accurate to 10%. The radial integrals for free ions were obtained from relativistic self-consistent Dirac-Slater wave functions as given by Lewis et al[26]; namely, $\langle r^2 \rangle_{5f} = 5.388 \times 10^{-17}\ cm^2$ and $\langle r^{-3} \rangle_{5f} = 5.300 \times 10^{25}\ cm^{-3}$. For a pure $^7F_0$ electronic state the reduced matrix element $\langle 20\|\alpha\|00 \rangle = 2/5\sqrt{3} = 0.23094$(Ref. 15) whereas for the intermediate coupled state obtained by diagonalizing the combined electrostatic and spin-orbit interaction matrices $\langle 20\|\alpha\|00 \rangle = 0.18857$ (Ref.27). For $LaCl_3:Am^{3+}$ the $^7F_2$ state lies

5328 cm^{-1} above the $^7F_0$ ground state,[18] and a comparable splitting should occur in an ethylsulfate lattice. When these values are substituted into Eq. 8 we obtain $-0.0032\ cm^{-1} = -0.000985\ cm^{-1}\ (1 - \sigma_2) + 0.000251\ cm^{-1}$ so that $1 - \sigma_2 = 0.285$ or $\sigma_2 = 0.715$. This value can easily be in error by 50%, but it agrees very well with the value $\sigma_2 = 0.73$ for the lanthanide analogue, Eu^{3+} (Ref. 20). Although this interpretation is not unique, it gives reasonable values for the parameters B_0^2, σ_2, and γ_∞. In particular, it seems clear that $(1 - \gamma_\infty)$ must have a value of $\approx 10^2$. A re-analysis of the $LaCl_3:Am^{3+}$ optical data would be especially helpful in establishing both B_0^2 and σ_2.

We next discuss the effect of the α-particle partial wave amplitudes and phases on the angular distribution.

The phase shifts in Eq. 1 are the sum of the intrinsic phases on the nuclear surface, which were assumed to be either 0 or π, plus the phase shifts that occur upon transmission through the combined Coulomb and quadrupole barriers. The intrinsic phases are taken from the microscopic shell model theory;[10] namely, the s, d, and g waves are all in phase but the i wave is out of phase. The Coulomb barrier phase shift difference for alpha decay is[28]

$$\sigma_{\ell+2} - \sigma_\ell = \tan^{-1} \frac{\eta}{\ell+1} + \tan^{-1} \frac{\eta}{\ell+2} \qquad (10)$$

where η is the argument of the Coulomb functions. For ^{241}Am the d wave lags the s wave by approximately 7° and the g wave lags the s wave by approximately 23.5°. The quadrupole phase shifts can be obtained only by numerical integration of the set of coupled differential equations that result from the consideration of the exchange of energy and angular momentum between the outgoing alpha particle

and the daughter nucleus.[29,30] Since these calculations have not yet been performed for ^{241}Am, the quadrupole phase shifts were taken to be zero. The quadrupole part of the barrier has the effect of retarding higher ℓ-waves with respect to the lower ℓ-waves if the waves are in phase at the nuclear surface. Therefore the quadrupole phase shifts for ^{241}Am would be additive to the Coulomb phase shifts except for the i wave which was not included in the analysis of the angular distribution because it is too weak to influence the results.

In order to compare theory with experiment we re-write Eq. 1 as

$$W(\Theta)_{expt.} = 1 + R\left[Q_2 A_2 B_2 P_2(\cos\Theta) + Q_4 A_4 B_4 P_4(\cos\Theta)\right] . \qquad (11)$$

Higher order Legendre polynomials are excluded for the decay of a spin 5/2 state. The factor R is an anisotropy reduction factor accounting for the fact that not all ^{241}Am nuclei are at rare-earth sites in the NES lattice. For the results reported here R is between 0.54 and 0.83. The solid curve in Fig. 1 was obtained using $P = -0.0033\ cm^{-1}$, $RA_2 = 0.54$ and $RA_4 = 0.05$. We want to point out that the shape of the experimental angular distribution curves rather than the absolute values are of importance. The competing requirements for a good nuclear orientation source were discussed in I. There are always radioactive nuclei that either are not at lattice sites or are so deeply imbedded in the crystal that the outgoing alpha particles are excessively scattered. These events contribute an isotropic background with the result that the full theoretical angular distribution is usually not achieved.

We next present three different estimates for the partial wave amplitudes. The resulting A_2 and A_4 coefficients are tabulated in Table II.

The fact that W(0) > 1 means that the s and d waves are in phase for ^{241}Am, in confirmation of the shell model calculations. Our experimental results do not establish the relative s-g wave phase (predicted to be positive), primarily because of the weakness of the g wave. Therefore in Table II we include the A_2 and A_4 values for both relative g wave phases.

In the theory of Bohr, Fröman, and Mottelson (BFM)[31] as it is usually applied the branching of an ℓ-wave is given by the product of (the square of a Clebsch-Gordan coefficient)) times (a calculated spherical barrier penetrability for the alpha group) times (the reciprocal of the hindrance factor averaged from neighboring even-even nuclei). The intensities resulting from the application of this method to ^{241}Am are given in Table III. A partial decay scheme for ^{241}Am is given in Fig. 2. The experimental intensities were taken from Nuclear Data,[32] and the band assignments were taken from Lederer et al.[33]

Numerical integration of the coupled differential equations for ^{233}U alpha decay performed by Chasman and Rasmussen (CR)[29] suggested that the relative intensity for the d wave to the ground state would be increased by 40% over the BFM predicted value. Although the application of this correction for other nuclei was never suggested by these authors, it has been successfully used in the analysis of the ^{243}Am α-γ angular correlation as will be mentioned later. This CR correction substantially alters A_2 as can be seen from Table II.

In the Mang shell model theory as applied by Poggenburg et al[10] the anisotropic barrier penetration was calculated using Fröman's method,[34] and assuming a realistic sloping inner barrier. In I it was found that the BFM intensities more closely fitted the NO data than did the Poggenburg intensities; however the BFM calculations had the advantage of the use of experimental ℓ-wave hindrance factors averaged from neighboring even-even nuclei. In contrast all of Poggenburg's transition probabilities were normalized with respect to

^{238}Pu and are thereby more model dependent. The shell model predicted intensities are given in Table IV. The $\ell = 6$ wave is included to illustrate its predicted weakness which justifies its exclusion.

Let us now try to choose the best A_2-A_4 pair given in Table II. The A_k coefficients obtained from the BFM theory and the shell model theory are very similar, and a choice of one over the other will be difficult. As expected the relative s-g wave phase influences A_4 primarily. Because the d wave intensity is fifty times greater than the g wave intensity, the a_2a_2 direct term in A_4 is five times larger than the a_0a_4 interference term. In most other cases the interference term dominates and hence the relative s-g wave phase determines the sign of A_4. For ^{241}Am A_4 is positive for either relative phase and therefore the magnitude of A_4 must be accurately determined in order to extract the phase. In order to decide whether this is feasible, let us consider the ratio A_4B_4/A_2B_2. From Table II, A_2 is between 8 and 18 times larger than A_4. Over the temperature range of our experiments $B_4/B_2 \approx 0.03$ at $1/T = 10\ K^{-1}$ and $B_4/B_2 \approx 0.22$ at $1/T = 90\ K^{-1}$. Therefore A_4B_4/A_2B_2 will never be larger than 0.025. We performed a least squares fit to our data with A_2 and A_4 as free parameters but could not get a satisfactory fit. We then tried an iterative procedure of fixing A_2 and leaving A_4 free, followed by fixing the resulting A_4 with A_2 free. Again the accuracy with which A_2 and A_4 were determined was not satisfactory. The basic problem is the small size of the quadrupole coupling constant and the resulting limited curvature that develops in the anisotropy curves at the lowest temperature.

The Chasman and Rasmussen correction to the d wave branching to ground was required to explain both the ^{253}Es NO[1] and the ^{243}Am unattenuated angular correlation.[8] The angular correlation (AC) results are more germane to the present discussion.

Although there are only limited results for ^{241}Am, extensive published results exist for ^{243}Am which has the same Nilsson ground state as ^{241}Am; namely, $K\pi[Nn_z\Lambda] = 5/2-[523]$, and a similar rotational band structure.

Following alpha decay, time-dependent hf fields develop because of the excitation of the electronic shells caused by both the change in nuclear charge and the approximately 100 keV of recoil energy given the daughter nucleus. These "after effects" have been considered by Thun[35] and by Mang.[36] An objective of α-γ AC experiments is to obtain an unattenuated correlation by eliminating the extranuclear fields during the intermediate state lifetime. The AC function is commonly written as

$$W(\theta) = \sum_k G_k(t) A_k' P_k(\cos\theta) \qquad (12)$$

where $G_k(t)$ is a time-dependent attenuation coefficient. As before the A_k' depend on the spins and multipolarities involved in the decays.

For the attenuated (5.486 MeV α - 59.54 keV γ) correlation from ^{241}Am Krohn *et al*[6] determined the upper limit of A_2' to be -0.36(2). The negative sign in itself implies that the s and d waves are in phase; a result that our experiments confirmed. For this cascade the $P_4(\cos\theta)$ term vanishes and therefore the relative s-g phase cannot be determined.

Asaro and Siegbahn[7] measured the correlation between alpha particles populating the 118 keV level of ^{239}Np and the de-exciting gamma rays in order to determine the relative d-g wave phase. Their results indicate that the phase is negative, but the positive phase could not be excluded.

For the unattenuated ($G_k = 1$) (5.275 MeV α - 75 keV γ) cascade in the decay

of ^{243}Am Falk et al[8] obtained $A_2' = -0.404(10)$. Using liquid sources Hutchinson[9] obtained $A_2' = -0.41(2)$ for this same cascade. The 75 keV level of the ^{239}Np daughter is the first member of the 5/2-[523] band and corresponds to the 59.54 keV level of ^{237}Np. The BFM theory predicts that $A_2' = -0.358$ while the CR correction gives $A_2' = -0.405$ in excellent agreement with experiment. The corresponding partial wave amplitudes are $a_2/a_0 = (+)0.47$ and $(+)0.56$ for the BFM theory without and with the CR correction respectively. In contrast Poggenburg gets $a_2/a_0 = +0.42$ which yields $A_2' = -0.33$, well outside the experimental error. The effect of the g wave on the theoretical A_2' was not considered by Falk et al; however, its inclusion alters A_2' by only 1% because of the low g wave intensity.

Rasmussen[37] pointed out differences in the d wave branching for the decay of the three odd-mass Am isotopes all of which have the same Nilsson ground state. Using the compilation of Ellis and Schmorak[38] we have calculated the ratio of the hindrance factor (HF) for the α-decay to the 9/2- state to the HF for decay to the 7/2- state. If these states were populated by pure d waves, BFM theory predicts the ratio to be $\langle \frac{5}{2}2\frac{5}{2}0 | \frac{7}{2}\frac{5}{2} \rangle^2 / \langle \frac{5}{2}2\frac{5}{2}0 | \frac{9}{2}\frac{5}{2} \rangle^2 = 2.857$. The experimental ratios are 3.50, 3.75 and 4.36 for ^{239}Am, ^{241}Am and ^{243}Am respectively. If the g wave contribution were subtracted from the experimental HFs, the above values would increase, thereby increasing the discrepancy between the BFM ratio and the experimental values. Because of the different HF ratios for ^{241}Am and ^{243}Am, there is no assurance that the CR correction found to be applicable to ^{243}Am will also be applicable to ^{241}Am. The observed trend of HF ratios with increasing neutron number is in the opposite direction to what would be expected. Since the g wave is becoming more highly hindered with increasing N, the HF ratios should decrease rather than increase. We have no explanation for the observed trend.

In general there is no justification for applying the CR correction to the relative $\ell=2$ wave intensity throughout the actinides. The BFM assumption that the K quantum number is a constant of motion has not been supported by coupled channel numerical integrations applied to the decay of ^{253}Es and ^{255}Fm.[39] The channel coupling which spoils the BFM branching ratios depends on the relative strengths of a number of coupling matrix elements. Although the d and g wave branching to the lower states in a rotational band is enhanced over the BFM theory estimates as a result of the channel coupling, the percentage enhancement is not always the same as that found by Chasman and Rasmussen for ^{233}U. In fact, AC experiments[40] on ^{249}Cf showed that the BFM theory overestimates the d wave intensity, a result which is unexpected.

We now briefly discuss the ^{255}Fm NO results. Paramagnetic resonance studies of Er^{3+}, the lanthanide analogue of Fm^{3+}, diluted in lanthanum ethylsulfate, yielded the hf interaction parameters $|A| = 0.0052(1)$ cm^{-1}, $|B| = 0.0314(1)$ cm^{-1} and $|P| = 0.0030(3)$ cm^{-1} (Ref. 41). For $|B|>|A|$ the nuclear magnetic substates are admixed except when $|k| = I + 1/2$ where $k = I_z + S_z$ where $S_z = \pm 1/2$. The levels labeled by + k and - k are degenerate except when k = 0. The ground state for a half integral nuclear spin is a singlet $(|1/2, -1/2\rangle - |-1/2, 1/2\rangle)/\sqrt{2}$, and a doublet lies closely above. The alignment may be regarded as being in a plane perpendicular to the crystalline c-axis, and the degree of alignment is relatively small.

The experimental α-particle angular distribution from ^{255}Fm nuclei aligned in NES is shown in Fig. 3. The statistical accuracy of the results is limited by the low degree of alignment, the mass of ^{255}Fm available (~ 200 disintegrations/m), and the short half-life. The shape of the anisotropy curve yields a value for

$|B|$ of 0.035(7) cm^{-1} or $|B|/k$ = 0.05(1) K. We could not determine the value of $|B|/|A|$, but as for Er^{3+}, the temperature dependence of W(O) establishes that the magnitude of B is greater than that of either A or P. The value of the anisotropy reduction factor R is approximately 0.8. In comparing theory to experiment the reader should note that B_2 is negative and B_4 is positive for non-axial alignment.

For non-axial alignment the counting rate along the c-axix decreases for a positive s-d phase. From Fig. 3 it is seen that this is the case. The solid curve in Fig. 3 was obtained using our value for $|B|$ with $|A| = 0$ and the relative amplitudes and phases given by Poggenburg[10] for the favored decay to the 7/2+[613] rotational band in ^{251}Cf. Poggenburg's predicted intensities and phases are given in Table V. The resulting A_k parameters are given in Table VI for both relative g wave phases. On the basis of NO experiments on ^{253}Es,[1] the negative relative phase should be correct. A partial decay scheme for ^{255}Fm, as derived from Asaro et al,[42] is given in Fig. 4.

In Table VII we list the intensities given by the BFM theory. The theoretical intensities were taken from Asaro et al,[42] but the d and g wave branching was modified by using the HFs given in the Table of Isotopes.[43] A striking difference between Tables V and VII is the factor of four difference in total g wave branching. This is reflected in the A_4 parameters given in Table VI. In order to simplify his calculations Poggenburg used a constant nuclear radius parameter and basis wave functions appropriate near the deformation $\eta = 5$. Although this approximation should be good for medium weight actinides, it should break down for the lightest and heaviest actinides. Therefore for ^{255}Fm we expect that the BFM branching rule may be more accurate than the values given by Poggenburg.

We could not determine the relative s-g wave phase because our 90° detector failed during the experiment. Even though the anisotropy is small, determination of the ratio $W(0)/W(\pi/2)$ would make it possible to decide among the four cases given in Table VI. In Table VI we have tabulated this ratio at $1/T = 90.5\ K^{-1}$ for a point source and a point detector.

IV. SUMMARY

The orientation of trivalent actinide elements in the neodymium ethylsulfate lattice is straight forward. The four elements Am, Cf, Es and Fm have been oriented in this way. It is difficult, however, to study α-particle angular distributions with precision. The results reported here for ^{241}Am and ^{255}Fm are sufficiently quantitative to establish that the s and d waves in the favored transitions are in phase, but they do not permit the determination of the relative s-g wave phase. The orientation data yielded definitive information about the electronic ground states of both Am^{3+} and Fm^{3+}. In $Am^{3+}(5f^6)$ as in $Eu^{3+}(4f^6)$, quadrupole coupling dominated the nuclear orientation, and the antishielded crystal field term A_2^0 was the main contributor to the electric field gradient. The data strongly support a large negative Sternheimer antishielding factor, $\gamma_\infty \approx -10^2$, and they also indicate a shielding constant $\sigma_2 \approx 0.7$, in good agreement with an earlier value for Eu^{3+}. In $Fm^{3+}(5f^{11})$, as in $Er^{3+}(4f^{11})$, the electronic ground-state in the ethylsulfate lattice has $|B| > |A|$.

ACKNOWLEDGEMENT

We are grateful to Drs. N. J. Stone and E. Matthias for their collaboration during the early stages of this research.

REFERENCES

† Work performed under the auspices of the U. S. Atomic Energy Commission.

1. A. J. Soinski, R. B. Frankel, Q. O. Navarro and D. A. Shirley, Phys. Rev. C2, 2379 (1970).

2. W. T. Carnall, S. Fried and F. Wagner, Jr., J. Chem. Phys. 58, 3614 (1973).

3. B. R. Judd, C. A. Lovejoy and D. A. Shirley, Phys. Rev. 128, 1733 (1962).

4. R. M. Sternheimer, Phys. Rev. 159, 266 (1967). See also R. E. Watson and A. J. Freeman, Phys. Rev. 135, A1209 (1964).

5. R. P. Gupta and S. K. Sen, Phys. Rev. A7 850 (1973) and S. K. Sen, private communication, 1973.

6. V. E. Krohn, T. B. Novey and S. Raboy, Phys. Rev. 105, 234 (1957).

7. F. Asaro and K. Siegbahn in E. Karlsson, E. Matthias and K. Siegbahn, editors, Perturbed Angular Correlations (North-Holland Publishing Co., Amsterdam, 1964), p. 233.

8. F. Falk, S. Törnkvist, J. E. Thun, K. Siegbahn and F. Asaro, Z. Physik 198, 106 (1967).

9. J. M. R. Hutchinson, Phys. Rev. 157, 1093 (1967).

10. J. K. Poggenburg, H. J. Mang and J. O. Rasmussen, Phys. Rev. 181, 1697 (1969) and J. K. Poggenburg, Jr., Lawrence Radiation Laboratory Report UCRL-16187 (1965) (unpublished).

11. Preliminary experiments were reported by D. A. Shirley, N. J. Stone and E. Matthias, Bull. Am. Phys. Soc. 10, 715 (1965).

12. A. Abragam and M. H. L. Pryce, Proc. Roy. Soc. (London) A205, 135 (1951).

13. A. J. Freeman and R. E. Watson, Phys. Rev. 132, 706 (1963).

14. R. M. Sternheimer, Phys. Rev. 95, 736 (1954).

15. R. J. Elliott, Proc. Phys. Soc. (London) 70B, 119 (1957).

16. B. D. Dunlap, G. M. Kalvius and G. K. Shenoy, Phys. Rev. Letters 26, 1085 (1971).

17. John B. Gruber, J. Chem. Phys. 35, 2186 (1961).

18. John G. Conway, J. Chem. Phys. 40, 2504 (1964).

19. William F. Krupke and John B. Gruber, J. Chem Phys. 46, 542 (1967).

20. J. Blok and D. A. Shirley, Phys. Rev. 143, 278 (1966).

21. D. Sengupta and J. O. Artman, Phys. Rev. B1, 2986 (1970).

22. W. T. Carnall, private communication, 1974.

23. H. Crosswhite, private communication, 1974.

24. B. R. Judd, Mol Phys. 2, 407 (1959).

25. T. E. Manning, M. Fred and F. S. Tomkins, Phys. Rev. 102, 1108 (1956).

26. W. Burton Lewis, Joseph B. Mann, David A. Liberman and Don T. Cromer, J. Chem. Phys. 53, 809 (1970).

27. We are grateful to Dr. N. Edelstein for providing the computer codes for this calculation.

28. S. Devons and L. J. B. Goldfarb, Handbuch der Physik (Springer-Verlag, Berlin, 1957) 42, p. 415.

29. R. R. Chasman and J. O. Rasmussen, Phys. Rev. 115, 1257 (1959).

30. John O. Rasmussen and Eldon R. Hansen, Phys. Rev. 109, 1656 (1958).

31. A. Bohr, P. O. Fröman and B. R. Mottelson, Dan. Mat. Fys. Medd. 29 no.10 (1955).

32. Nuclear Data B6, 635 (1971).

33. C. M. Lederer, J. K. Poggenburg, F. Asaro, J. O. Rasmussen and I. Perlman, Nucl. Phys. 84, 481 (1966).

34. Per Olof Fröman, Mat. Fys. Skr. Dan Vid. Selsk. 1, no.3. (1957).

35. J. E. Thun in Hans van Krugten and Bob van Nooijin, editors, Angular Correlations in Nuclear Disintegration (Rotterdam University Press, The Netherlands, 1971), p. 78.

36. H. J. Mang, Ibid., p. 103.

37. J. O. Rasmussen, private communication, 1974.

38. Y. A. Ellis and M. R. Schmorak, Nuclear Data B8, 345 (1972).

39. A. J. Soinski, E. A. Rauscher and J. O. Rasmussen, Bull. Am. Phys. Soc. 18, 768 (1973) and A. J. Soinski, D. G. Raich, J. O. Rasmussen and E. A. Rauscher, contribution to 167th American Chemical Society National Meeting, March 31 - April 5, 1974, Abstract no. NUCL.

40. F. Falk, A. Linnfors, B. Orre and J. E. Thun, Physica Scripta 1, 13 (1970).

41. G. S. Bogle, H. F. Dufus and H. E. D. Scovill, Proc. Phys. Soc. (London) A 65, 760 (1952).

42. F. Asaro, S. Bjørnholm and I. Perlman, Phys. Rev. 133, 3291 (1964).

43. C. M. Lederer, J. M. Hollander and I. Perlman, Table of Isotopes, 6th Edition (John Wiley and Sons, Inc., N.Y. , 1967).

44. I. Ahmad, private communication, 1974.

Table I. Experimental ^{241}Am in neodymium ethylsulfate alpha particle angular distribution as a function of inverse temperature.

$1/T\ (K^{-1})$	W(O)	$W(\pi/2)$
10.8(3)	1.060(7)	0.969(9)
15.0	1.104(8)	0.939(10)
19.3(17)	1.132(5)	0.933(7)
31.7(6)	1.193(8)	0.883(9)
43.5(2)	1.274(8)	0.859(10)
55.6	1.330(12)	0.822(13)
74.0	1.412(10)	0.781(10)
88.5	1.460(24)	0.748(16)
90.5	1.500(14)	0.736(17)

Table II. Coefficients A_2 and A_4 for the ^{241}Am in NES angular distribution function $W(\Theta) = 1 + R[A_2Q_2B_2P_2(\cos\Theta) + A_4Q_4B_4P_4(\cos\Theta)]$.

	A_2	A_4
BFM theory, s and g waves in phase	0.7747	0.0756
BFM theory, s and g waves out of phase	0.7477	0.0483
BFM theory, Chasman and Rasmussen correction, s and g waves in phase	0.8668	0.1032
BFM theory, Chasman and Rasmussen correction, s and g waves out of phase	0.8390	0.0770
Mang theory, s and g waves predicted to be in phase	0.7838	0.0847
Mang theory but with s and g waves out of phase	0.7398	0.0397

Table III. Intensities for partial waves in ^{241}Am favored alpha transitions to the first excited rotational band in ^{237}Np according to the method of Bohr, Froman and Mottelson.[31] Numbers in parentheses have been modified by the "Chasman and Rasmussen correction."[29]

E_f(keV)	I_f^π	s	d	g	i	$\sum$(%)	Measured intensity (%)
59.54	5/2-	72.56 (67.76)	14.29 (19.08)	0.004		86.85	85.5
102.96	7/2-		10.81	0.017	0.0004	10.83	12.6
158.52	9/2-		1.81	0.018	0.0024	1.83	1.6
226.0	11/2-			0.006	0.0037	0.010	0.015
304.8	13/2-			0.0006	0.0019	0.0025	0.002

Table IV. Intensities and phases for partial waves in ^{241}Am favored alpha transitions to the first excited rotational band in ^{237}Np as calculated by Poggenburg.[10]

I_f^π	s	d	g	i	$\sum$ (%)	Measured intensity (%)
5/2-	72.74	14.36	0.011		87.12	85.5
7/2-		10.70	0.045	-0.0004	10.74	12.6
9/2-		1.76	0.046	-0.0025	1.81	1.6
11/2-			0.0158	-0.0052	0.0210	0.015
13/2-			0.0015	-0.0020	0.0035	0.002

Table V. Intensities and phases for partial waves in ^{255}Fm favored alpha transitions to ^{251}Cf as calculated by Poggenburg.[10]

I_f^{π}	s	d	g	i	$\sum$(%)	Measured intensity (%)[44]
7/2+	82.47	10.28	-0.092	-0.0003	92.84	93.4(2)
9/2+		5.231	-0.197	-0.0024	5.43	5.05(7)
11/2+		0.651	-0.132	-0.0052	0.78	0.62(1)
13/2+			-0.0338	-0.0045	0.0383	0.110(5)
15/2+			-0.0027	-0.0017	0.0044	0.013(2)

Table VI. Coefficients A_2 and A_4 for the ^{255}Fm in neodymium ethylsulfate alpha particle angular distribution function and the ratio $W(0)/W(\pi/2)$ at $1/T = 90.5\ K^{-1}$.

	A_2	A_4	$W(0)/W(\pi/2)$
BFM theory, s and g waves out of phase	0.596	-0.0397	0.434
BFM theory, s and g waves in phase	0.695	0.1566	0.400
Poggenburg calculation based on shell model theory, s and g waves predicted to be out of phase	0.634	0.0003	0.413
Poggenburg calculation but with s and g waves in phase	0.700	0.1242	0.390

Table VII. Intensities for partial waves in ^{255}Fm favored alpha transitions to the first excited rotational band in ^{251}Cf according to the method of Bohr, Fröman and Mottelson.[31]

E_f(keV)	I_f^π	s	d	g	$\sum$(%)	Measured intensity (%)[44]
106	7/2+	83.4	9.6	0.23	93.2	93.4(2)
165	9/2+		4.89	0.50	5.39	5.05(7)
238	11/2+		0.62	0.35	0.97	0.62(1)
325	13/2+			0.086	0.086	0.110(5)
421	15/2+			0.0066	0.0066	0.013(2)

FIGURE CAPTIONS

Fig. 1. ^{241}Am in neodymium ethylsulfate (NES) alpha particle angular distribution at 0° and 90° with respect to the crystalline c-axis as a function of the inverse temperature.

Fig. 2. Partial decay scheme for ^{241}Am as adapted from references 32 and 33.

Fig. 3. ^{255}Fm in NES alpha particle angular distribution at 0° with respect to the crystalline c-axis as a function of the inverse temperature.

Fig. 4. Partial decay scheme for ^{255}Fm as adapted from reference 42.

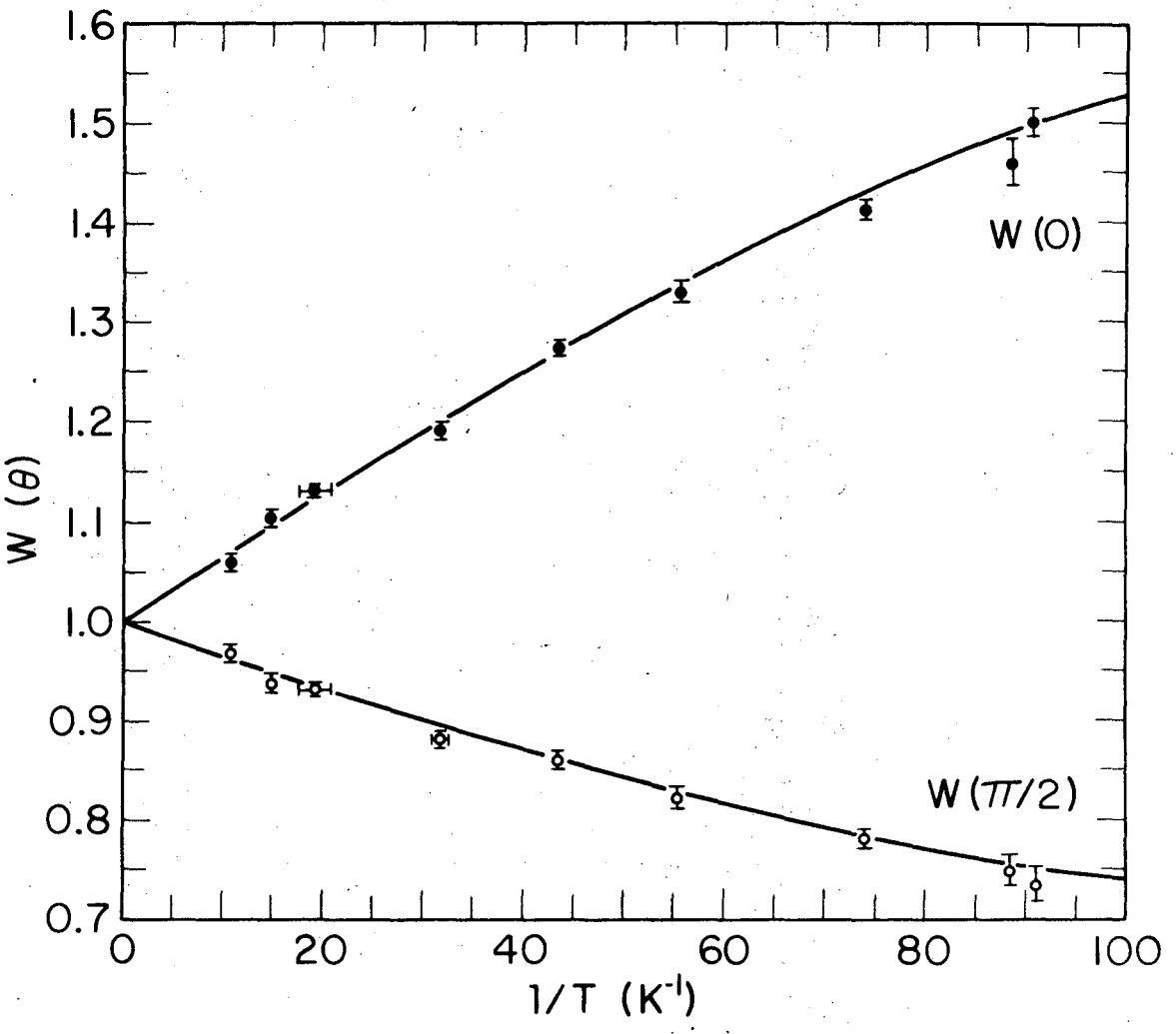

XBL 745-3063

Fig. 1.

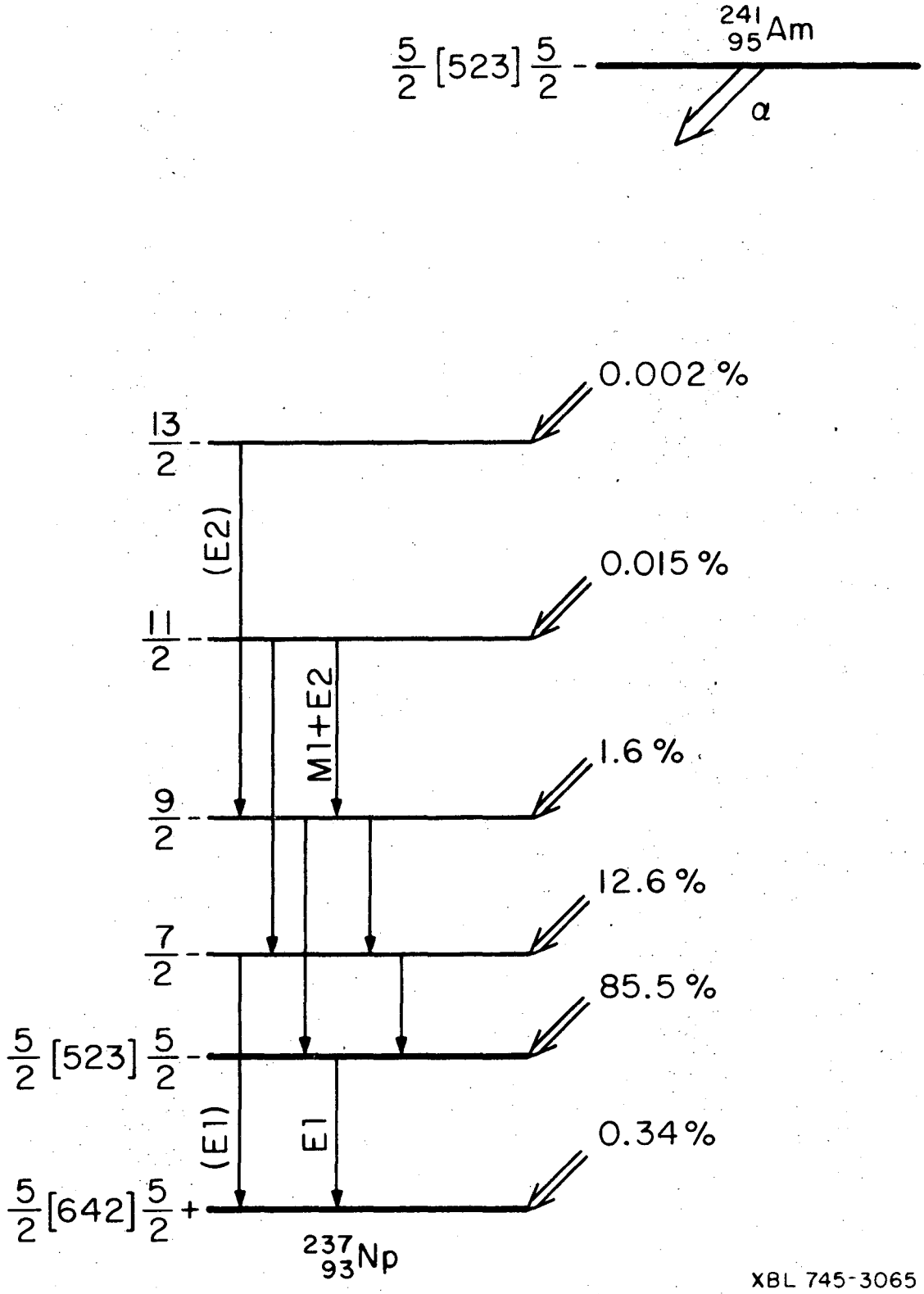
241 95 Am
5/2 [523] 5/2 -
α
0.002 %
13/2 -
(E2)
0.015 %
11/2 -
M1+E2
1.6 %
9/2 -
12.6 %
7/2 -
85.5 %
5/2 [523] 5/2 -
(E1)
E1
0.34 %
5/2 [642] 5/2 +
237 93 Np
XBL 745-3065

Fig. 2.

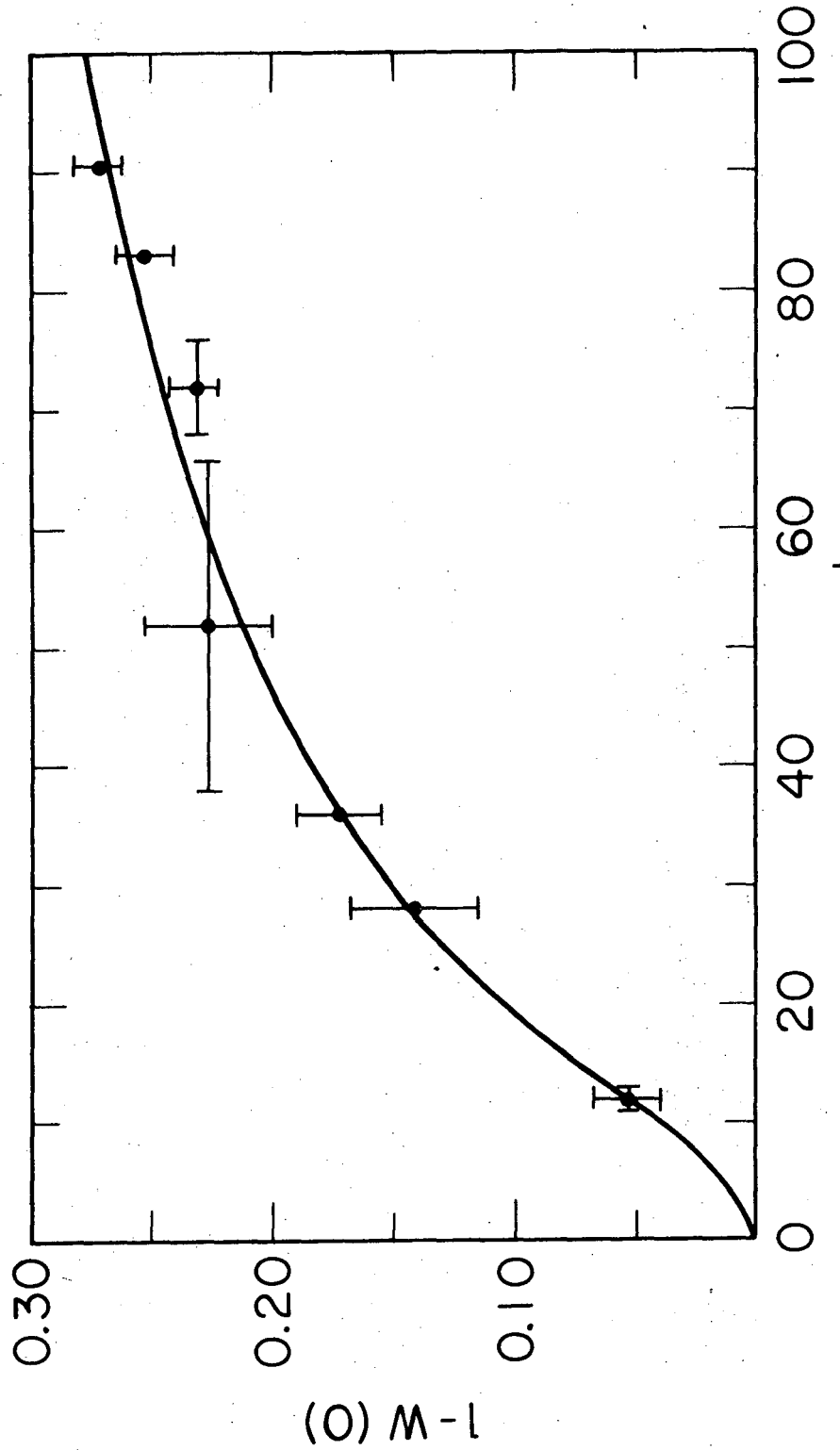

XBL 745-3064

Fig. 3.

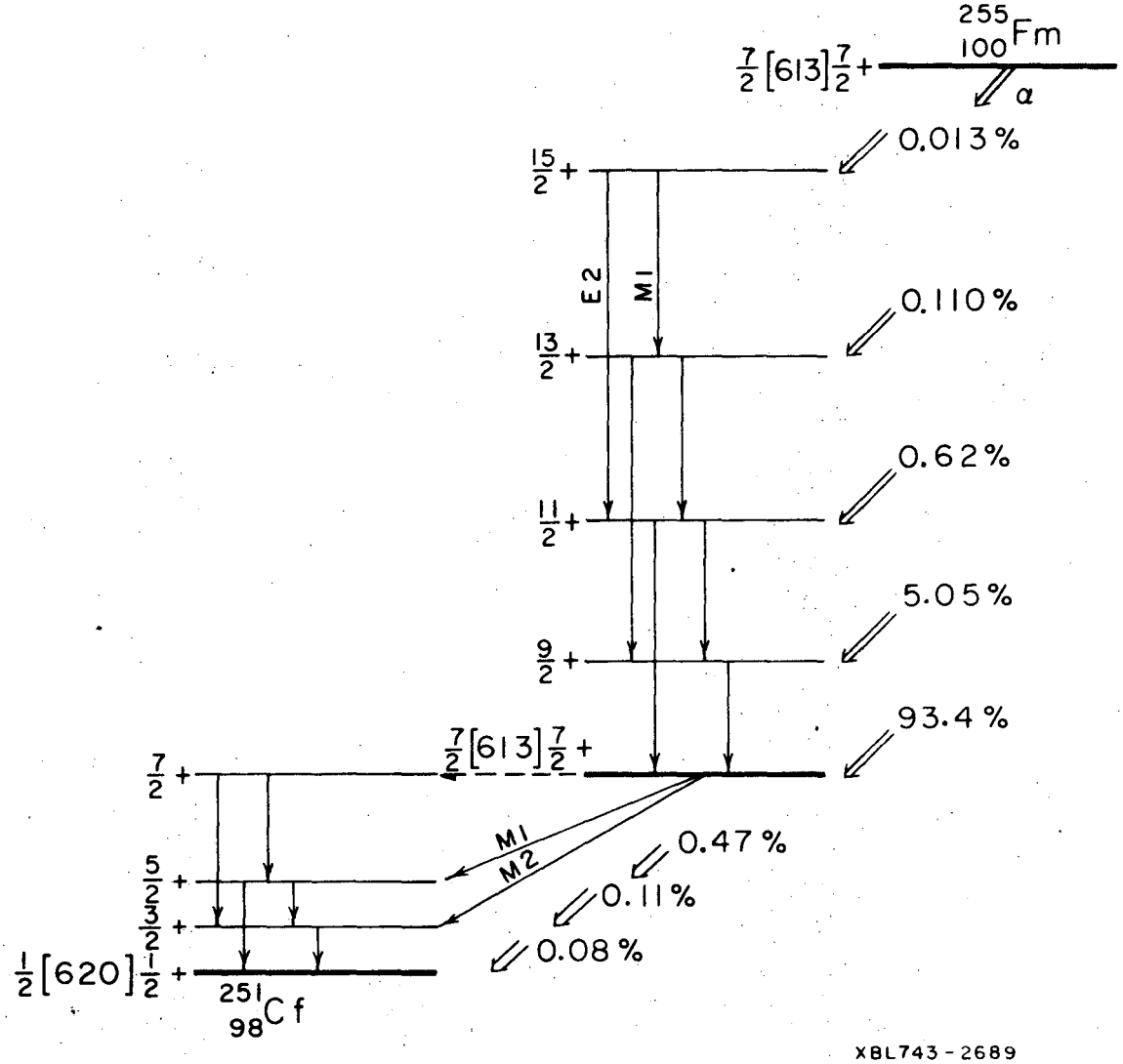
$\frac{7}{2}[613]\frac{7}{2}+$ $^{255}_{100}Fm$
α
0.013 %
$\frac{15}{2}+$
E2
M1
0.110 %
$\frac{13}{2}+$
0.62 %
$\frac{11}{2}+$
5.05 %
$\frac{9}{2}+$
93.4 %
$\frac{7}{2}[613]\frac{7}{2}+$
$\frac{7}{2}+$
M1
M2
0.47 %
$\frac{5}{2}+$
0.11 %
$\frac{3}{2}+$
0.08 %
$\frac{1}{2}[620]\frac{1}{2}+$
$^{251}_{98}Cf$
XBL743-2689

Fig. 4.

TECHNICAL INFORMATION DIVISION
LAWRENCE BERKELEY LABORATORY
UNIVERSITY OF CALIFORNIA
BERKELEY, CALIFORNIA 94720